Determination of hoop direction effective elastic moduli of non-circular profile, fiber reinforced polymer composite sewer liner pipes from lateral ring compression tests

Gergely Czél[1,2] and Dénes Takács[3]

[1]Department of Polymer Engineering, Faculty of Mechanical Engineering, Budapest University of Technology and Economics

H-1111 Budapest, Műegyetem rkp. 3. Hungary

[2]MTA–BME Research Group for Composite Science and Technology, Budapest University of Technology and Economics

H-1111 Budapest, Műegyetem rkp. 3. Hungary

[3]Department of Applied Mechanics, Faculty of Mechanical Engineering, Budapest University of Technology and Economics

H-1111 Budapest, Műegyetem rkp. 3. Hungary

Corresponding author: Czél G. E-mail: czel@pt.bme.hu,

tel.: +36 1 463 1487, fax: +36 1 463 1527

Abstract

A new material property determination method is presented for the calculation of effective elastic moduli of non-circular ring specimens cut from filament wound oval profile polymer composite sewer liner pipes. The hoop direction elastic moduli was determined using the test results obtained from ring compression tests, which is a very basic setup, and requires no special equipment. Calculations were executed for many different oval profiles, and diagrams were constructed, from which the cross section dependent C_{eff} constants can be taken. The new method was validated by the comparison of tests and finite element analysis

results. The calculation method and the diagrams are essential design tools for engineers, and a big step forward in sizing non-circular profile liner pipes .

Keywords: Composite pipe, Ring compression test, Glass fiber, Polyester, Finite element method

1. Introduction

High performance composite materials consisting of thermosetting polymer matrix (mainly epoxy, vinylester or unsaturated polyester resins) and reinforcing fibers (carbon, glass or aramide fibers) show high strength, acceptable elastic modulus, low density and high chemical resistance. These special properties have made fiber reinforced polymer composites suitable for the underground piping industry, where low maintenance need of these materials is an additional benefit [1]. Glass fiber reinforced unsaturated polyester (GF/UP) pipes and vessels have been manufactured for more than four decades, and applied successfully in food industries, and in underground water and sewerage piping [2]. Glass and carbon fiber reinforced composites are also suitable for repairing pressure pipes [3]. Major advantages of polymer composite pipes compared to steel ones are low weight, which decreases construction and transportation costs, corrosion and chemical resistance [4] that reduces maintenance costs and extends the lifetime of the pipes. Composite pipes have higher strength and stiffness compared to thermoplastic polymer pipes (PE, PP, PVC), which gives higher pressure resistance and load bearing capacity, and finally allows the designer to use lower wall thicknesses.

Composite pipes are manufactured mainly by filament winding and rotational casting, and they can be operated under gravity or internal pressure. The former manufacturing technology is more common for high performance pipes mainly because the anisotropic mechanical properties of the pipe material can be fitted to the loads by changing the winding angle [5],[6].

In the early stage of sewerage piping, various pipe cross sections were built from stones or bricks with masonry technique. Notable amount of these pipes are older than a hundred years, and is in need for rehabilitation. Effective ways of repairing underground pipes are the trenchless lining technologies, where the surface traffic is only slightly affected by the construction works [7]. The most common sewer pipe lining technologies are “cured in

place pipe" lining (CIPP), where a preformed hose impregnated by uncured resin is pulled into the section to be repaired, and then filled and cured with pressurized steam; and the "short pipe process", where prefabricated (cured) liner pipe sections are pulled or pushed into the old pipe. Both technologies are capable of lining non-circular profile pipes. In this study we are focusing on pre-fabricated filament wound sewer lining pipes with special symmetric oval cross sections which consist of three circular arc sections with different radii.

Besides their advantageous special properties, polymer composites show some uncommon behavior compared to conventional structural materials (metals). Most of the unusual properties, such as temperature dependent properties [8],[9], degradation and water absorption [10],[11] are due to the macromolecular structure of the polymer matrix material. Composites also show uncommon damage modes in comparison with tough materials, such as various fracture types [12] due to their fiber reinforced laminated structure. The fibrous reinforcing structure of the composite parts causes anisotropy in the material properties, which makes the design process more difficult. There is a significant need for research in the field of structural design of sewer liners [13]. Researchers are developing better sizing methods which require more accurate material properties. Because of the uncommon material behavior, hundreds of possible fiber–matrix combinations and sensitive curing process [14], testing is even more important in case of composite materials than in case of metals. The most effective tests should be executed on the composite parts themselves, because the reinforcing fiber structure can be kept unaffected in this way.

Testing of pipe materials is always problematic, because it is difficult to fabricate standard specimens from a pipe. Longitudinal tensile or compression specimens have curvatures in the transverse direction that is why special adhesive materials and tabs are needed to make the clamping areas even. This way the tensile properties can be evaluated using EN 1393 using a special cross sectional area calculation method developed in a former study [15]. Only curved specimens can be taken from the circumferential direction of the pipe, on which flexural tests can be executed according to EN 13566-4. The mechanical properties in the circumferential direction can be determined from circumferential tensile tests (EN 1394) and from ring compression tests (EN 1228). The cited standards often give methods for determining product properties instead of material properties. Product properties are suitable for quality control and other comparative tests, but cannot be applied for comparing different materials and product types. Ring compression test is a very basic setup (Fig. 1), which does not modify the reinforcing structure of the pipe and for which no special equipment is needed.

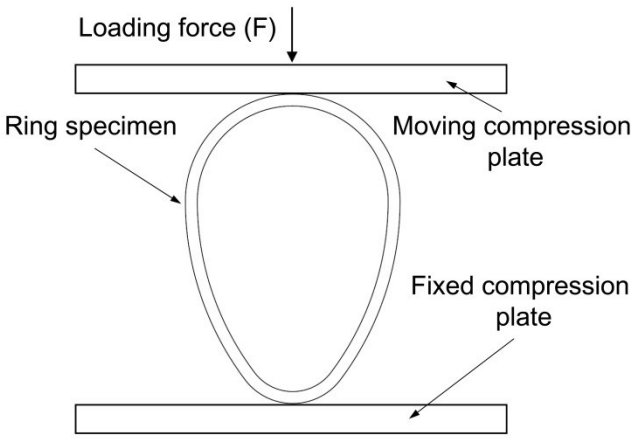

Fig. 1 Ring compression test setup with regular egg-shaped profile specimen

Applying an appropriate evaluation method, the hoop direction effective elastic moduli (E_{eff}) of the tested pipe materials, which is the most important design parameter, can be calculated from ring compression tests even for non-circular cross sections. The static design methods of sewer liner pipes, including non-circular profile ones [16],[17], operating under gravity, consider the groundwater or grout injection pressure as outer pressure loading. The hoop direction effective elastic modulus of the pipe material is therefore the most important input parameter for the design methods. In the following paragraphs, the shape of the examined cross sections and the new test evaluation method will be explained in details.

The aim of this paper is to provide design engineers with a simple test and a quick evaluation method which is capable of determining the hoop direction effective elastic modulus, the most important mechanical property of non-circular profile composite pipes. The proposed simple test can also be used for quality and general product control and it is applicable to a wide variety of pipe cross-sections.

2. Examined oval profiles

In this study the authors focused on oval profiles that can be described with closed symmetric convex curves which consist of four arcs with three different radii. The four sections connect with common tangents, and form a continuously differentiable curve. The mentioned oval curves have four basic types which can be seen on Fig. 2.

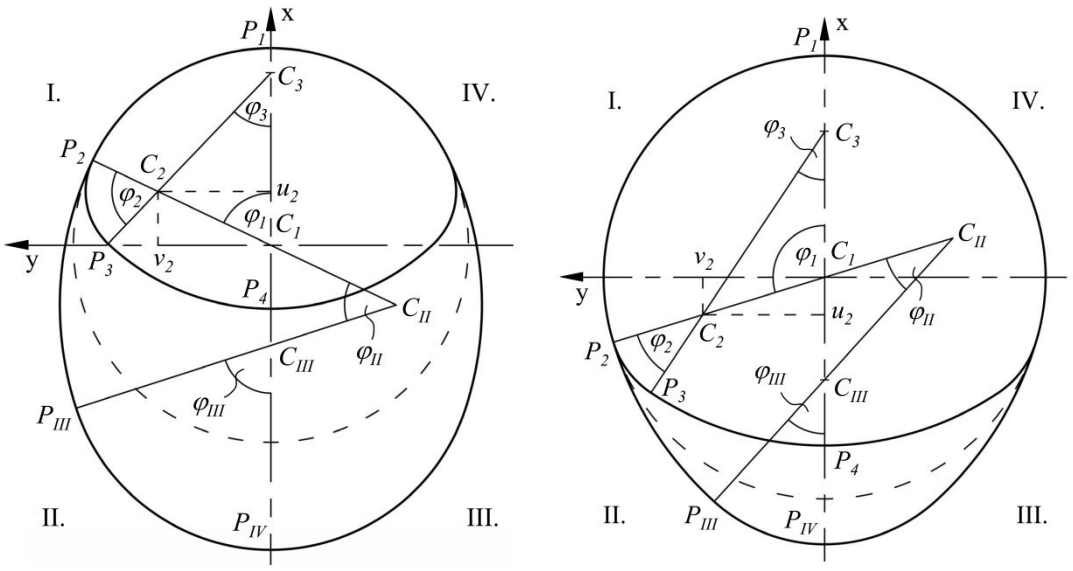

Fig. 2 Basic types of examined oval curves, a) the first circle sections are fully in the I. quadrant, b) the first circle sections are in the I. and the II. quadrants. (Dashed lines show the circles with C_1 centers)

- type 1.: The first arc is fully in the I. quadrant and the center of the second arc (C_2) is also in the I. quadrant (Fig. 2 a), upper profile).
- type 2.: The first arc is also fully in the I. quadrant but the center of the second arc (C_{II}) is in the III. quadrant (Fig. 2 a), lower profile).
- type 3.: The first arc is in the I. and the II. quadrants and the center of the second arc (C_2) is in the II. quadrant (Fig. 2 b), upper profile).
- type 4.: The first arc is in the I. and the II. quadrants and the center of the second arc (C_{II}) is in the IV. quadrant (Fig. 2 b), lower profile).

A special oval profile is the regular egg-shaped cross section, which was very common in the early decades of sewerage piping because of its advantageous flow and ergonomic properties. The first egg-shaped sewers were constructed in London in 1846, and later from the 1870s they were used also in Germany. Up till now hundreds of kilometres of egg-shaped sewers can be found under the big cities of Europe such as London, Paris, Brussels, Berlin, Dresden, Hamburg, Vienna, Budapest etc. In case of a combined (communal wastewater and rainwater) sewer, the egg-shaped profile provides deeper flow during the dry periods, due to the narrow lower part of the section, than an equivalent circular profile and this way it prevents sedimentation. In case of wet weather, the section has enough spare capacity to transport stormwater. On the other hand, egg-shape is very similar to the figure of the human body (e.g. on all fours) that is why a 1200x700 mm section or even smaller can be man-

accessible. An additional benefit of egg-shaped sewers was, during the construction works, that a narrower trench was suitable for laying them, than the one for an equivalent circular profile pipe (with equal cross-sectional area). Egg-shaped profile pipes are mainly used for repair and recovery of deteriorated pipelines, because manufacturing various non circular profiles for new construction is not cost effective enough, and sizes cannot be easily standardized. Even nowadays polymer composite liner pipes are manufactured in high volume with this non-circular profile which is a borderline case between type 1-2 and type 3-4 because C_2 is on the horizontal axis (see Fig. 3). The main geometrical parameters of the regular egg-shaped profile are the following: $R_1 = \left|\overline{C_1P_1}\right| = R_m$, $R_2 = \left|\overline{C_2P_2}\right| = 3R_m$, $R_3 = \left|\overline{C_3P_3}\right| = R_m/2$, φ_1=90°, φ_2=36.87°, φ_3=53.13°, where R_m is the characteristic mean radius of the profile (see also Fig. 4). These parameters characterize an oval profile with a height of $3R_m$ and a width of $2R_m$. Detailed mechanical calculations were performed on regular egg-shaped profiles, and then a generalization step was taken with which the calculation can be applied on any oval profiles from the type mentioned above.

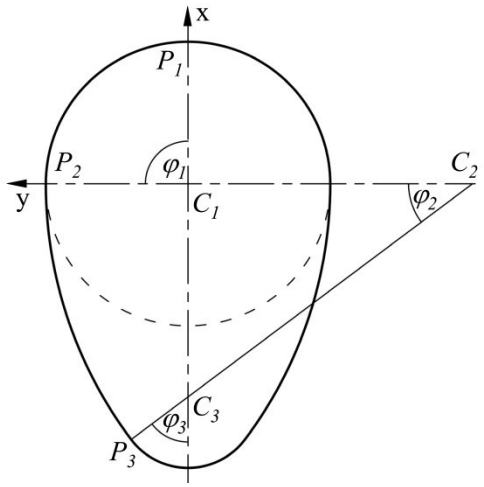

Fig 3 Regular egg-shaped profile

3. Results and discussion

In the following paragraph a new evaluation method of the ring compression test is shown for the regular egg-shaped profiles, and then the results are generalized with suitable geometrical parameters.

3.1. Calculation for regular egg-shaped profiles

The elastic deformation of thin-walled structures is usually analysed with Timoshenko's shell theory [18]. However, in case of the investigated compression test, one half of the non-circular ring specimen can simply be modelled with a curved beam. The following assumptions were made during the analysis:

1. The material shows linearly elastic behaviour, which is acceptable at small strains necessary for elastic modulus determination.
2. The cross sections of the beam remain planes that are perpendicular to the neutral axis of the beam during the deformation.
3. The material shows identical elastic properties in case of tensile and compression loading.

The above mentioned assumptions are necessary for the calculations, and reasonable for composites with high fibre volume fraction. As the elastic moduli tests are executed under small displacements, the assumptions are acceptable, and no notable errors are generated by using them.

Fig. 4 shows the mechanical model of a regular egg-shaped profile ring under ring compression test alignment. As the profile is symmetric about its vertical axis, it is enough to examine one half of the profile. The neglected half of the profile was replaced with the internal forces (F_A, M_A, F_B, M_B), which kept the whole structure in equilibrium.

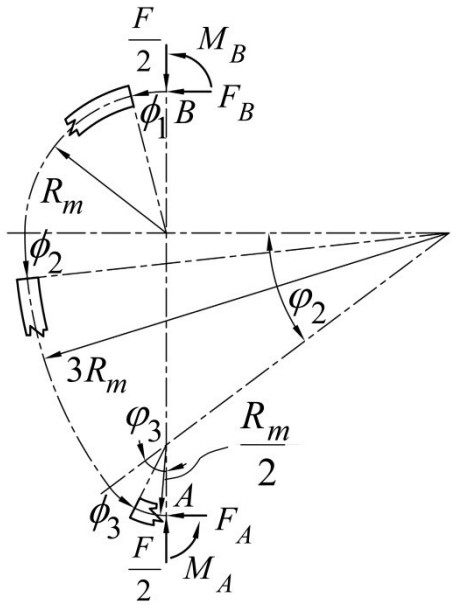

Fig. 4 Mechanical model and notations for calculating the effective elastic modulus (E_{eff}) of a regular egg-shaped ring specimen under ring compression loading

The concentrated force $F/2$ is considered as the external load for the half of the profile, acting from the compression plates. The equilibrium equations of the examined structure can be written with equations (1) and (2).

$$F_A + F_B = 0 \tag{1}$$

$$M_A + M_B + F_B \cdot 3R_m = 0 \tag{2}$$

To determine the internal forces of the structure, further equations are needed. The missing equations can be written using the work theorem of statics. First, the general form of the strain energy has to be written paying attention only to the dominant forces (equation (3)).

$$U = \int_{(l)} \frac{M_h^2(s)}{2IE_{eff}} \mathrm{d}s + \int_{(l)} \frac{N^2(s)}{2AE_{eff}} \mathrm{d}s \tag{3}$$

where $M_h(s)$ and $N(s)$ are the bending and normal stress resultant functions along the arc length, respectively, I is the moment of inertia of the model beam (ring specimen) calculated with respect to the axis of bending, A is the cross-sectional area of the model beam. As the regular egg-shaped profile consists of three arcs, the bending and the normal stress resultant functions can be written as a piecewise function, which is characterized by three sections. Functions are given by equations (4)-(9).

$$M_{h1}(\phi_1) = M_B + F_B \cdot R_m \cdot (1 - \cos\phi_1) - \frac{F}{2} \cdot R_m \cdot \sin\phi_1 \tag{4}$$

$$M_{h2}(\phi_2) = M_B + F_B \cdot (R_m + 3R_m \cdot \sin\phi_2) - \frac{F}{2} \cdot (R - 3R_m \cdot (1 - \cos\phi_2)) \tag{5}$$

$$M_{h3}(\phi_3) = M_B + F_B \cdot \left(2{,}5R_k + \frac{R_m}{2} \cdot \cos(\varphi_3 - \phi_3)\right) - \frac{F}{2} \cdot \frac{R_m}{2} \cdot \sin(\varphi_3 - \phi_3) \tag{6}$$

$$N_1(\phi_1) = -\frac{F}{2} \cdot \sin\phi_1 - F_B \cdot \cos\phi_1 \tag{7}$$

$$N_2(\phi_2) = -\frac{F}{2} \cdot \cos\phi_2 + F_B \cdot \sin\phi_2 \tag{8}$$

$$N_3(\phi_3) = -\frac{F}{2} \cdot \sin(\varphi_3 - \phi_3) + F_B \cdot \cos(\varphi_3 - \phi_3) \tag{9}$$

where $0 \le \phi_1 \le \frac{\pi}{2}$, $0 \le \phi_2 \le \varphi_2$ and $0 \le \phi_3 \le \varphi_3 = \frac{\pi}{2} - \varphi_2$. Using the functions above, the strain energy can be written as functions of the corresponding angles (10).

$$U = \int_0^{\frac{\pi}{2}} \frac{M_{h1}^2(\phi_1)}{2IE_{eff}} R_m \cdot \mathrm{d}\phi_1 + \int_0^{\varphi_2} \frac{M_{h2}^2(\phi_2)}{2IE_{eff}} 3R_m \cdot \mathrm{d}\phi_2 + \int_0^{\varphi_3} \frac{M_{h3}^2(\phi_3)}{2IE_{eff}} \frac{R_m}{2} \cdot \mathrm{d}\phi_3 + \\ + \int_0^{\frac{\pi}{2}} \frac{N_1^2(\phi_1)}{2AE_{eff}} R_m \cdot \mathrm{d}\phi_1 + \int_0^{\varphi_2} \frac{N_2^2(\phi_2)}{2AE_{eff}} 3R_m \cdot \mathrm{d}\phi_2 + \int_0^{\varphi_3} \frac{N_3^2(\phi_3)}{2AE_{eff}} \frac{R_m}{2} \cdot \mathrm{d}\phi_3 \tag{10}$$

According to the theorem of Castigliano [19], the partial derivatives of the strain energy with respect to the internal forces are zero and the partial derivative with respect to the active forces gives the displacement (*f*) in the direction of the selected force. Using this theorem, equations (11)-(13) can be written.

$$\frac{\partial U}{\partial F_B} = 0 \tag{11}$$

$$\frac{\partial U}{\partial M_B} = 0 \tag{12}$$

$$\frac{\partial U}{\partial \left(\frac{F}{2}\right)} = f \tag{13}$$

The system of equations (1), (2) and (11)-(13) can be solved, and the internal forces (F_A, M_A, F_B, M_B) and the effective elastic modulus (E_{eff}) of the pipe material can be calculated. The analytical solution leads to a complicated formula of E_{eff}, in which the geometrical parameters and the force-displacement pairs of the test results appear. To obtain a simpler formula, the normal stress resultant function was neglected in the strain energy. Using the simplified formula of strain energy resulted in only 0.06 % error in the E_{eff} values calculated from our experimental data. In this simplified case, the effective moduli of the pipe material can be calculated from ring compression test results using formula (14).

$$E_{eff} = 0.1691 \cdot \frac{R_m^3}{I} \cdot \frac{\Delta F}{\Delta f} \tag{14}$$

where $I = l \cdot t^3 / 12$ is the moment of inertia of the pipe wall calculated with respect to the axis of bending, where l is the width of the ring specimen, t is the wall thickness of the specimen. Finally, $\Delta F / \Delta f$ is the initial ramp of the force-vertical displacement curve of the ring compression test.

3.2. Calculation for general oval profiles

Writing the bending resultant functions for a general oval profile with the notations of Figures 2, 3 and 4, equations (15)-(17) are given for the three different arcs.

$$M_{h1}(\phi_1) = M_B - \frac{F}{2} \cdot R_1 \cdot \sin\phi_1 + F_B \cdot R_1 \cdot (1 - \cos\phi_1) \tag{15}$$

$$\begin{aligned} M_{h2}(\phi_2) = M_B - \frac{F}{2} \cdot (R_1 \cdot \sin\varphi_1 + R_2 \cdot \sin(\varphi_1 + \phi_2) - R_2 \cdot \sin\varphi_1) + \\ F_B \cdot (R_1 \cdot (1 - \cos\varphi_1) + R_2 \cdot \cos\varphi_1 - R_2 \cdot \cos(\varphi_1 + \phi_2)) \end{aligned} \tag{16}$$

$$\begin{aligned} M_{h3}(\phi_3) = M_B - \frac{F}{2} \cdot (R_1 \cdot \sin\varphi_1 - R_2 \cdot \sin\varphi_1 + R_2 \cdot \sin(\varphi_1 + \varphi_2) - R_3 \cdot \sin\varphi_3 + R_3 \cdot \sin(\varphi_3 - \phi_3)) + \\ F_B \cdot (R_1 \cdot (1 - \cos\varphi_1) + R_2 \cdot \cos\varphi_1 + R_2 \cdot \cos\varphi_3 + R_3 \cdot \cos(\varphi_3 - \phi_3) - R_3 \cdot \cos\phi_3) \end{aligned} \tag{17}$$

where $0 \le \phi_1 \le \varphi_1$, $0 \le \phi_2 \le \varphi_2$ and $0 \le \phi_3 \le \varphi_3 = \pi - \varphi_1 - \varphi_2$.

If the bending resultant function is considered in the strain energy only, the calculation of the regular egg-shaped profile can be repeated, and the effective modulus E_{eff} can be calculated for the general oval profile by formula (18).

$$E_{eff} = C_{eff} \cdot \frac{R_1^3}{I} \cdot \frac{\Delta F}{\Delta f} \tag{18}$$

where the coefficient C_{eff} is typical of the investigated profile (for example, in case of a regular egg-shaped profile C_{eff}=0.169). R_1 is the first mean radius of the profile (in case of a regular egg-shaped profile R_1=R_m).

Oval profiles can be described with four independent geometrical parameters, namely, R_1, R_2, φ_1, φ_2. Obviously, all the parameters are necessary to calculate the elastic modulus E_{eff} of the pipe material but the classification of the oval profiles and the calculation of the coefficient C_{eff} can be done with the help of the quotients R_2/R_1, φ_2/φ_1 and the value of φ_1. This means that C_{eff} is a hyper surface in the (R_2/R_1, φ_2/φ_1, φ_1) three dimensional parameter space, which can be represented by its contour curves in plane. Actually, the quotient φ_2/φ_1 was fixed and the contours of C_{eff} values in the (R_2/R_1, φ_1) plane were constructed. For example, Fig. 5 shows the contours for φ_2/φ_1=0.40966 which is characteristic of the regular egg-shaped profiles.

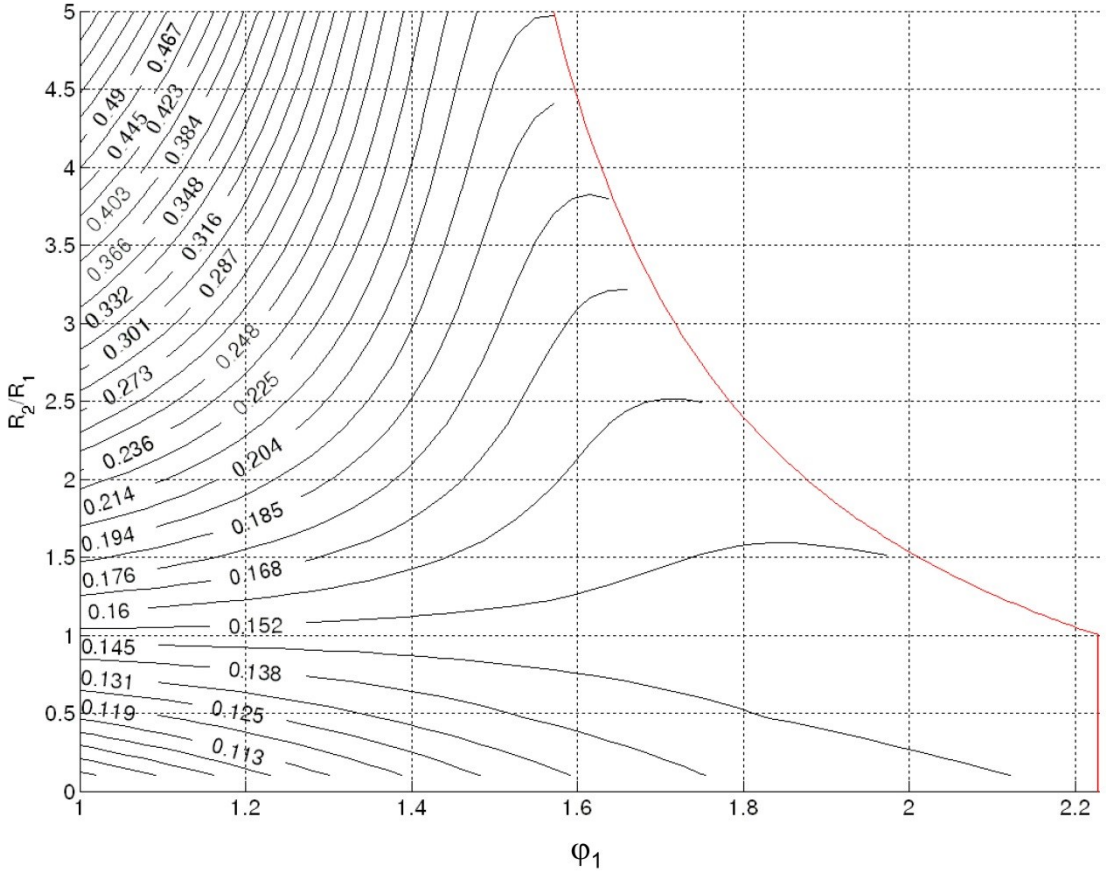

Fig. 5 C_{eff} values on the R_2/R_1-φ_1 plane for φ_2/φ_1=0.40966 which is characteristic of the regular egg-shaped profiles

Boundary curves in Fig. 5 shows the geometrical boundaries of the examined profile, which are given by equations (19)-(20).

$$\varphi_1 < \frac{\pi}{1+\frac{\varphi_2}{\varphi_1}} \tag{19}$$

$$\frac{R_2}{R_1} < \frac{1}{1-\cos\varphi_2 - \sin\varphi_2 \cdot \cot\varphi_1} \tag{20}$$

The vertical line (equation (19)) shows that the sum of the three angles (φ_1, φ_2, φ_3) is always π. The upper (curved) boundary (equation (20)) is coming from the definition of the examined oval profiles. The contour curves similar to the ones in Fig. 5 can be constructed for different values of φ_2/φ_1, and C_{eff} values can be calculated for each possible oval profile.

The constructed contour curves are very useful for designer engineers because an essential material property, namely the hoop direction effective elastic modulus (E_{eff}) can be

calculated from a simple ring compression test for any oval profile using them. Therefore, several figures were constructed and some of them were added to the Appendix for different values of φ_2/φ_1. As an extreme case of the oval profiles, circular profile can be taken into account, which can be characterized by R_2/R_1=1. For this special case, C_{eff}=0.14866 independently from the values of the other parameters. The circular case is present in all constructed contour diagrams at R_2/R_1=1. The design engineers can find the right chart using the geometrical parameters of the examined profile, and the necessary C_{eff} value can be obtained by interpolation.

3.3. Verification of the new method

The developed effective modulus calculation method was applied to ring compression test results and verified by comparing the experimental load-displacement graphs to those obtained from a Finite Element Analysis (FEA) using the experimental effective moduli.

Quasi-static ring compression tests (see Fig. 1) were executed on three egg-shaped profile (see Fig. 3) ring specimens cut from a filament wound glass fiber reinforced unsaturated polyester composite pipe with fiber volume fraction v_f=53.9±2.2 % between stiff, flat, parallel steel compression plates at 6 mm/min cross-head speed on a Zwick Z050 type 50 kN rated computer controlled universal test machine. The nominal geometric properties of the tested rings were the following: characteristic mean radius: R_m=80 mm, nominal wall thickness: t=2.4 mm, width: l=40 mm, cross- sectional height: h=3R_m=240 mm, cross-sectional width: b=2R_m=160 mm. Each rings were compressed three times until the displacement of the upper compression plate reached 10 mm. The obtained nine test curves were aggregated into an average curve for easier comparison to model results. The effective elastic moduli of the specimens calculated with the developed method using equation (14) can be seen in Table 1. The initial slopes of the displacement- compression force curves ($\Delta F / \Delta f$) were determined graphically. Finally mean and standard deviation were calculated from all nine calculated hoop direction effective moduli values, which was E_{eff}=35.76±0.87 GPa.

Specimen number	Number of compression tests	Nominal wall thickness	Characteristic mean radius	Ring width	Hoop direction effective elastic modulus
-	-	[mm]	[mm]	[mm]	[GPa]
1	3	2.4	80	40	35.85±0.7
2					35.99±0.6
3					35.44±1.4

Table 1. Geometry and calculated effective elastic moduli of the tested specimens. Each average and standard deviation was calculated from the results of three tests executed on the same specimen.

Ring compression tests were simulated using the finite element method (FEM) in Abaqus software. Finite element model of the ring specimens were created assuming isotropic and linearly elastic properties. The above calculated average effective elastic modulus and an estimated Poisson's ratio ν=0.3 were used during the material property definition. Although it is well known, that filament wound pipes exhibit different elastic properties in hoop and axial direction, the assumption of isotropy is acceptable, because no significant stress and deformation was present during the initial stage of the tests in the axial direction. The effect of the applied Poisson's ratio on the results were analyzed in the reasonable range and found to be negligible. Quadratic 20 node brick elements (C3D20 type) were applied in a structured mesh (i.e. two layers of 1.2 mm edge size cubic elements through the pipe wall thickness). A convergence study, presented in a previous paper [20] for the same geometry and similar but orthotropic material, where the number of elements through the thickness was varied from one to eight indicated that two quadratic elements through the thickness provides accurate results with reasonable computation time. Therefore the same mesh structure was adopted here. Hard and frictionless contact was defined between the elastic ring section and the rigid compression plates. The ring compression test was simulated by applying equal increments of vertical displacement up to 10 mm on the upper compression plate and integrating the reaction force on the same rigid body as an output. The model was capable to represent the hoop direction elastic behavior of the ring specimens under the ring compression loading in the above mentioned 10 mm vertical displacement range. The geometry of the modeled ring was the same as that of the test specimens.

Fig. 6. shows the average compression test curve, and the result of the finite element analysis. Although the diagram shows that the results agree very well, a deviation analysis was performed. Relative absolute deviations (D) were calculated at 10 equally spaced displacement values using equation (21), and an average was calculated: D_{av}=1.65%±0.3%.

$$D = \frac{|F_{FEA} - F_{test}|}{F_{FEA}} \tag{21}$$

where F_{FEA} is the calculated and F_{test} is the measured compression force.

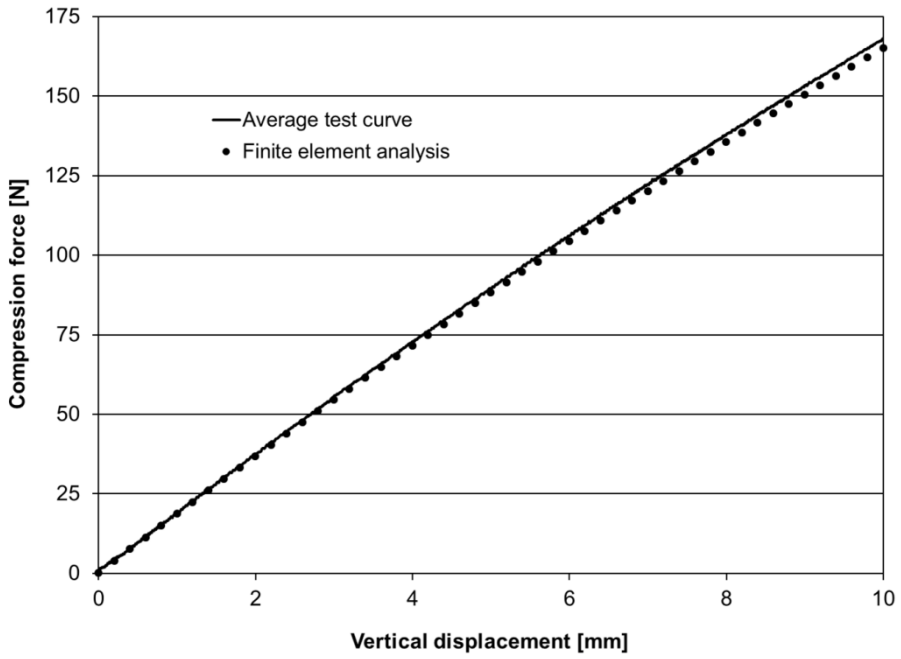

Fig. 6 Comparison of the average of compression test results and finite element analysis

According to the diagram of Fig. 6 and the calculated average of relative deviations (D_{av}) it can be stated, that the new hoop direction effective modulus calculating method is accurate enough to be used in the engineering practice.

4. Conclusions

A novel method was presented for determining the hoop direction effective elastic modulus of filament wound oval profile polymer composite pipes from ring compression test results. A detailed calculation was shown for regular egg-shaped profile rings to determine the C_{eff} constant, which is characteristic of the cross section, and a generalization was done using appropriate geometrical constants and running programmed calculations for several types of general oval profiles. This way, the design engineers can calculate the effective elastic moduli (E_{eff}) of various pipe materials from the results of simple compression tests of rings cut from any oval profile pipe. The new test evaluation method was verified by executing tests, and modeling the compression tests with the finite element method. The results obtained from the

tests and modeling, agreed well, proving that the method is capable of calculating the effective elastic modulus accurately enough for engineering practice. Using the new method, engineers can perform quick and accurate sizing of the pipes assuring safe operation, saving material and energy. The presented test and evaluation method is essential, because accurate prediction of material properties of composite materials before manufacturing is difficult. This is the reason, why testing is a vital part of the design process of composite materials.

Appendix

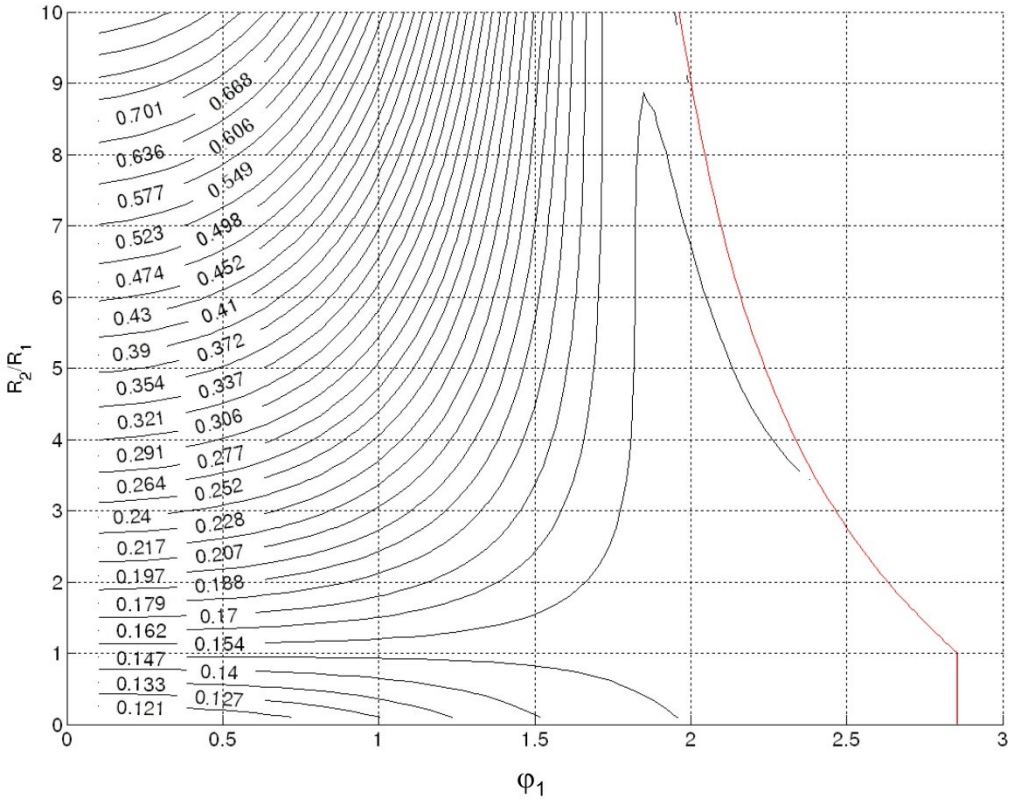

Fig. A. 1 C_{eff} values on R_2/R_1-φ_1 plane for φ_2/φ_1**=0.1**

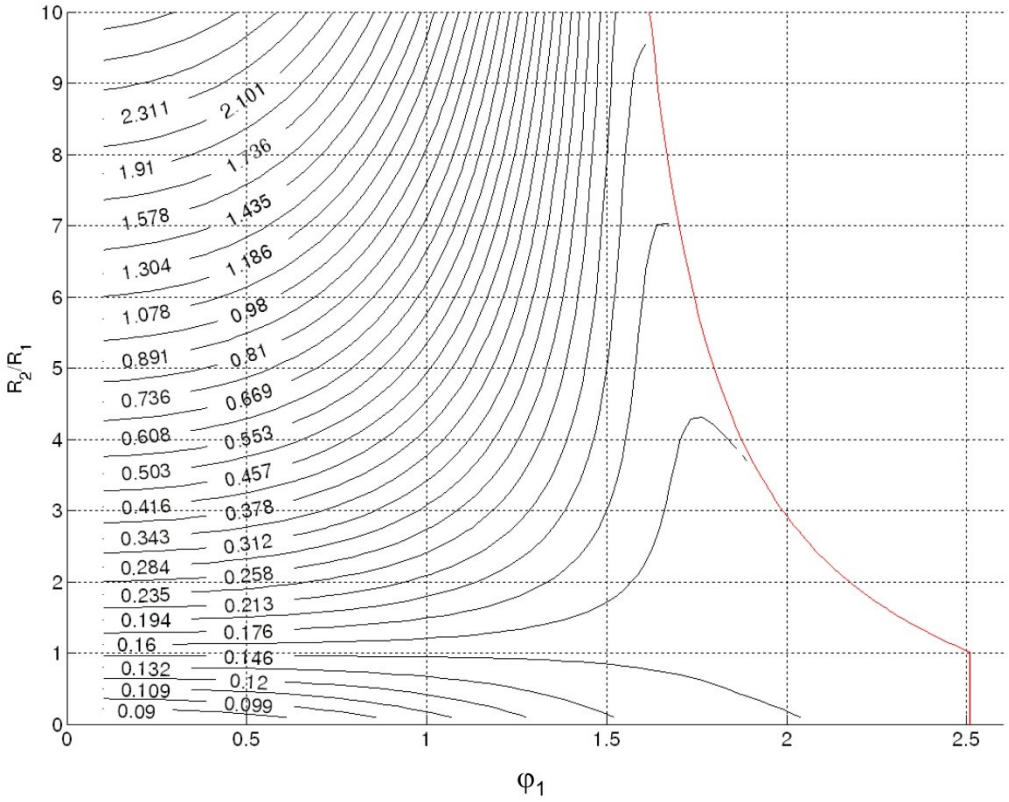

Fig. A. 2 C_{eff} values on R_2/R_1-φ_1 plane for φ_2/φ_1**=0.25**

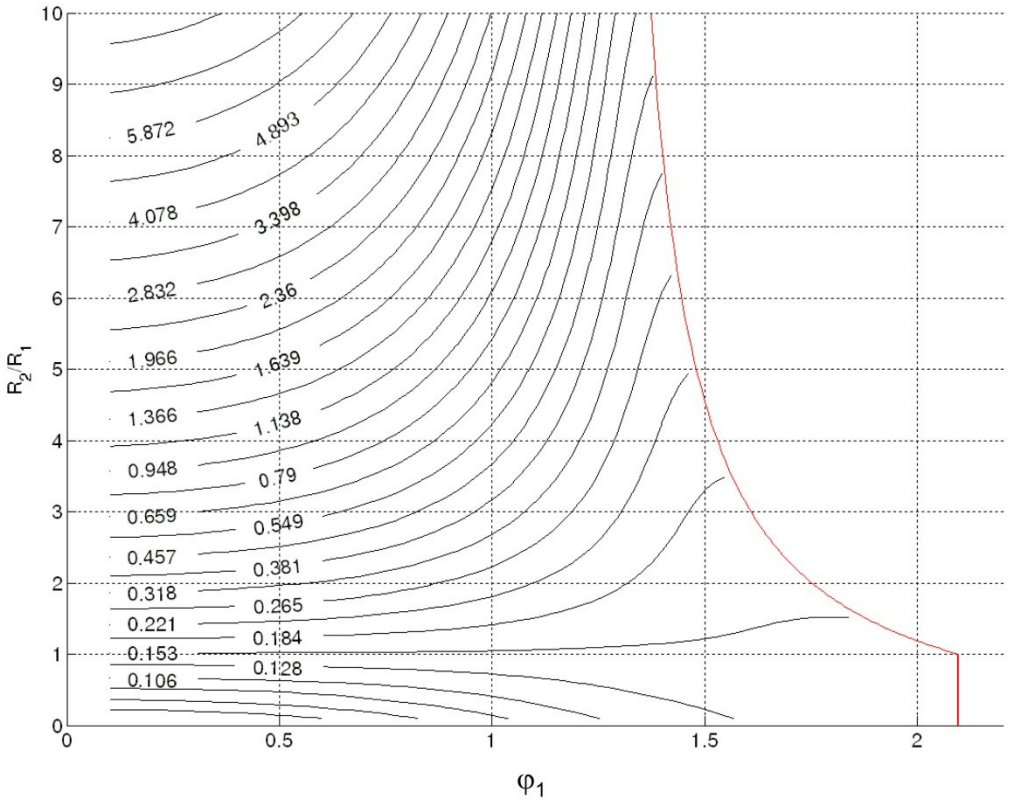

Fig. A. 3 C_{eff} values on R_2/R_1-φ_1 plane for φ_2/φ_1**=0.5**

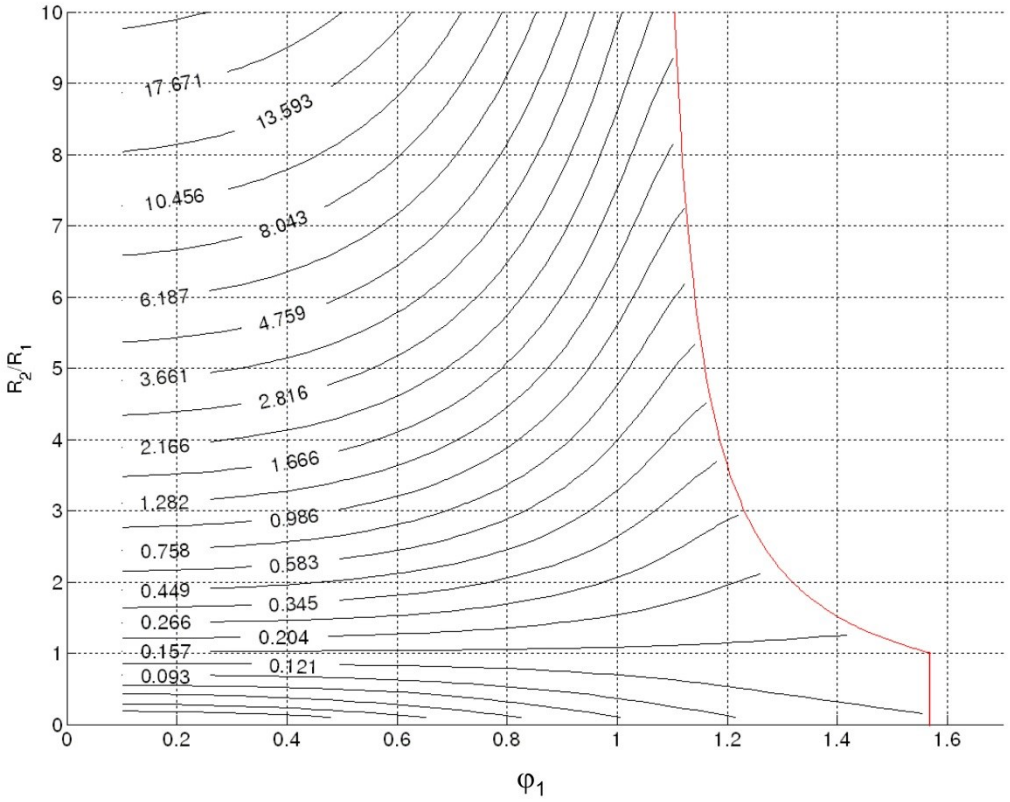

Fig. A. 4 C_{eff} values on R_2/R_1-φ_1 plane for $\boldsymbol{\varphi_2/\varphi_1=1}$

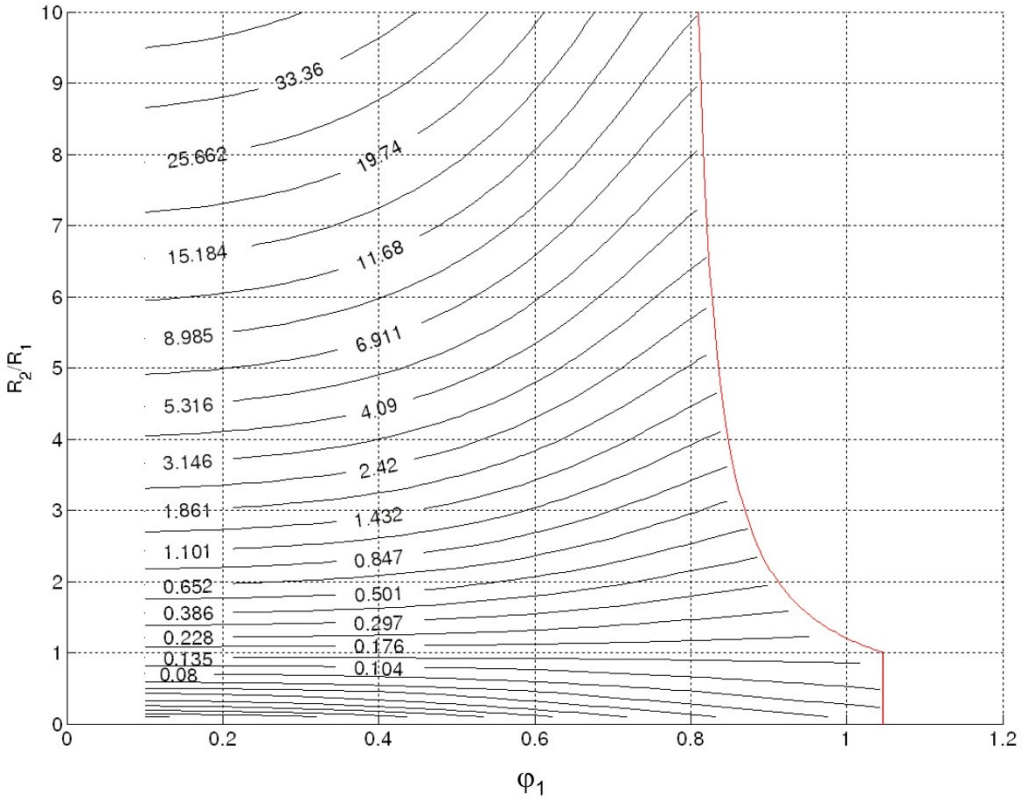

Fig. A. 5 C_{eff} values on R_2/R_1-φ_1 plane for $\boldsymbol{\varphi_2/\varphi_1=2}$

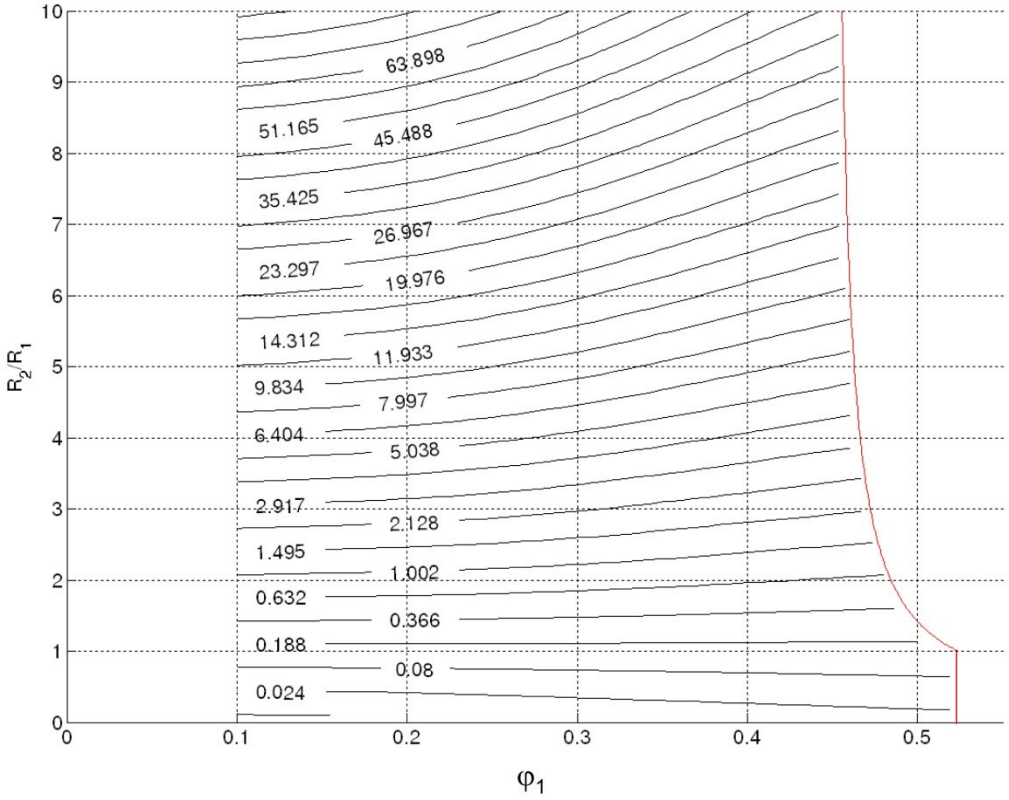

Fig. A. 6 C_{eff} values on R_2/R_1-φ_1 plane for $\boldsymbol{\varphi_2/\varphi_1=5}$

Acknowledgement

This work was supported by the Hungarian Ministry of Economics through grant GVOP–2004–3.1.1 and by the Hungarian National Development Agency through the Central Hungarian Operational Programme KMOP-2008-1.1.1 applications. This work is connected to the scientific program of the 'Development of quality-oriented and harmonized R+D+I strategy and functional model at BME' project. This project is supported by the New Széchenyi Plan (Project ID: TÁMOP-4.2.1/B-09/1/KMR-2010-0002). The authors acknowledge Hodács Composites Co. Ltd. for manufacturing the test-pipes.

References

[1] Lukács J. Dimensions of Lifetime Management. Mater Sci Forum 2005;473-474:361-368.

[2] Stein D. Rehabilitation and maintenance of drains and sewers. Berlin: Ernst & Sohn; 2001.

[3] Duell JM, Wilson JM, Kessler MR. Analysis of a carbon composite overwrap pipeline repair system. Int J Pres Ves and Pip 2008;85:782-788.

[4] Paul NJ, Hasan Ibrahim Al Hosani, El Masri A. Use of GRP material in power and desalination plants. Desalination, 1998;120:83-88.

[5] Hull D, Spencer B. Effect of winding angle on the failure of filament found pipe. Compos 1978;9:263-271.

[6] Soden PD, Kitching R, Tse PC, Tsavalas Y, Hinton MJ. Influence of winding angle on the strength and deformation of filament-wound composite tubes subjected to uniaxial and biaxial loads. Compos Sci Tech 1993;46:363-378.

[7] Ma Baosong, Najafi M. Development and applications of trenchless technology in China. Tunn Undergr Sp Tech 2008;23:476-480.

[8] Nakamura R, Goda K, Noda J, Ohgi J. High temperature tensile properties and deep drawing of fully green composites. Express Polym Lett 2009;3:19-24.

[9] Bakaiyan H, Hosseini H, Ameri E. Analysis of multi-layered filament-wound composite pipes under combined internal pressure and thermomechanical loading with thermal variations. Comp Struct 2009;88:532-541.

[10] Abacha N, Kubouchi M, Sakai T. Diffusion behavior of water in polyamide 6 organoclay nanocomposites. Express Polym Lett 2009;3:245-255.

[11] Czél G, Czigány T. Study of moisture absorption and mechanical properties of glass fiber / polyester composites – effects of specimen geometry and preparation. J Comp Mater 2008;42:2815-2827.

[12] Romhány G, Szebényi G. Interlaminar crack propagation in MWCNT/fiber reinforced hybrid composites. Express Polym Lett 2009;3:145-151.

[13] Boot JC, Gumbel JE. Research requirements in support of renovation of pressure and non-pressure pipes. Tunn Undergr Sp Tech 2007;22:515-523.

[14] Cheng J, Li J, Zhang JY. Curing behavior and thermal properties of trifunctional epoxy resin cured by 4, 4'-diaminodiphenyl sulfone. Express Polym Lett 2009;3:501-509.

[15] Czél G, Czigány T. Development and analysis of filament wound new composite pipes made of glass fibre reinforced 3P resin. Macromol Symp 2006;239:232-244.

[16] Thépot O. Structural design of oval-shaped sewer linings. Thin- Walled Struct 2001;39:499-518.

[17] Thépot O. A new design method for non-circular sewer linings. Trenchless Technol Res 2000;15:25-41.

[18] Timoshenko S, Woinowsky-Krieger S. Theory of plates and shells. New York: Mc Graw-Hill; 1959.

[19] Beer FP, Johnston ER, DeWolf JT. Mechanics of Materials. London: Mc Graw-Hill Inc.; 1992.

[20] Czél G, Czigány T. Finite element method assisted stiffness design procedure for non-circular profile composite wastewater pipe linings. Comp Struct 2014;112:78-84.